Impedance Array Studies of Mammalian Cell Growth

Duc D. Nguyen and Michael M. Domach
Department of Chemical Engineering, Carnegie Mellon University
5000 Forbes Avenue, Pittsburgh, PA 15217

Xiaoqiu Huang and David W. Greve
Department of Electrical & Computer Engineering, Carnegie Mellon University
5000 Forbes Avenue, Pittsburgh, PA 15217

ABSTRACT

Functional genomic studies and drug candidate testing both require high throughput, parallel experimentation to screen for variable cellular behaviors. Here we present the use of impedance sensing electrode array where each site is comparable to the area spanned by a few cells. The electrical signal from each sensing site provides information not only on cell "presence," but also on the extent of cell attachment to the substrate. Data will be presented on the signals provided by mouse fibroblasts growing on 9 similar sized electrodes. In the absence of cells, each electrode's impedance was found to depend as expected on electrode size and frequency. More notably, the impedance increased up to four-fold when fibroblasts attached and spread out over time. These findings suggest that such impedance sensors can detect cell "presence" as well as the extent of cell attachment to the substrate. Finite element simulation shows a good agreement with experimental results.

From a technological perspective, impedance sensors could play a role in automating cell proliferation assays. Alternately, in structures with many sensors and sparse cell coverage, cell tracking and motility experiments may be potentially conducted. Finally, it may be possible to use such impedance measurements to screen mutants and malignant cells as well as effectors for altered adhesion prior to employing more demanding methods.

KEY WORDS impedance sensors, sensing array, fibroblasts, finite element simulation

INTRODUCTION

Light-based experimental methods (e.g. interference microscopy) now exist that allow for cell-substrate interaction to be investigated in a quantitative way. Arrays of microelectrode impedance sensors have emerged as a new method for quantitatively measuring cell-substrate interaction (Tiruppathi et al., 1992; Ehret et al. 1997). Electrical sensor arrays may present several advantages over traditional methods. First, 100s to 1000s of sensing sites can be measured almost in "real time" when thin film transistors that are embedded underneath each sensing site are used as addressing devices. This capability can automate data acquisition as well as provide high throughput and high time-resolution. Secondly, impedance is a frequency-dependent quantity; hence, the signal-frequency pattern might be used as signature for a cell type. In addition, cellular responses to drugs or cytotoxic substances that optical methods may not easily detect may be observed. Third, when sensing sites are small enough, an array of impedance sensors can be used in conjunction with a stage-controlled microscope in order to track individual cells. Each sensor detects cell presence on its surface. The electrical signal can then drive the microscope stage to the located cell position. Overall, electrical device may prove to be an additional tool for drug discovery and other applications.

In this paper, we will describe a simple structure that contains 9 similar sensing sites and one common counter electrode. The purpose of this study is to gain a basic understanding of how impedance sensors work, and gain some understanding of how impedance measurements relate to the nature of cell-surface interactions. First, background on impedance measurements and the basics of cell adhesion will be provided. Impedance measurements without cells are then discussed. We will present results that show that cell proliferation can be detected by impedance sensors.

BACKGROUND

In this section, we briefly describe the characteristics of electrodes immersed in ionic liquids and also the effects of cells, which are adhered to the electrode. This discussion focuses on the small-signal impedance

measured between a small sensing electrode and a large reference electrode.

The impedance of electrodes in ionic liquids has been rather extensively investigated. When a solid object is immersed into an ionic solution, ions in the solution can react with the electrode and the solid ions from the electrode can enter the solution, leading to complex reactions at the interface. Eventually, electrochemical equilibrium is established at the interface. The net result is the development of a charge distribution at the interface with an associated electric potential distribution. The combined model of Helmholtz-Gouy-Chapman-Stern is the commonly accepted model describing the charge distribution at the electrode interface, which is shown in Figure 1.

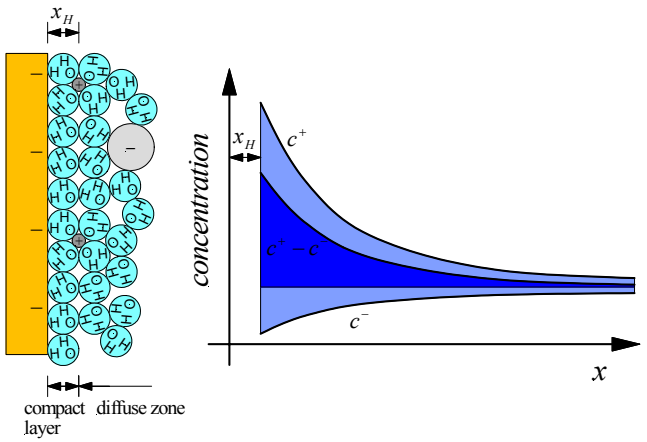

Fig. 1 A schematic representation of electrified metal electrode-ionic solution interface, and ion concentration at the interface. A compact layer next on the metal surface is Hemlholtz layer (x_H). The region away from the Helmholtz plane is known as the diffuse layer. An electrical double layer is created as a result of all the processes at the interface.

The current flowing through the electrified interface will encounter resistance R_{ct} caused by the electron transfer at the electrode surface and impedance Z_W due to limited mass diffusion from the electrode surface to the solution. As the result, in the equivalent circuit representing the electrode solution interface, the electron transfer resistance R_{ct} is in series with the mass diffusion limited impedance Z_W. As the current spreads out to the bulk solution, the electrode has a solution conductivity determined series resistance, represented as spreading resistance R_S in the equivalent circuit (Figure 2).

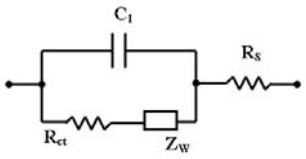

Fig. 2 Equivalent circuit of the electrode-ionic solution interface. C_I is interfacial capacitance, Z_W is Warburg impedance, R_{ct} is charge transfer resistance at the interface, and R_S is spreading resistance of ionic solution.

At the frequencies of interest in this work (f = 100 - 10^6 Hz), there is no conduction current through the cells due to the high resistivity of the plasma membrane. When cells attach and spread out on the gold electrode, they alter the current path and consequently the effective area. Figure 3 shows adhered cells on a gold electrode passively blocking current path. As the results, measured electrode impedance is increased by an amount, which depends on the cell size, the cell-electrode gap, and the measurement frequency.

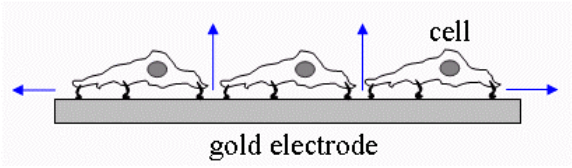

Fig. 3 Presence of cells on gold electrode passively block current path. Plasma membrane of the cells is highly insulated, therefore the current is forced to move outwardly through the gap between the cell and the electrode surface. Blue arrows are current flow directions.

The impedance change caused by cells has been calculated analytically using a simplified model (Giaever & Keese, 1991) and we have performed finite element simulations in order to obtain further insight (Huang et al., submitted to IEEE Sensors). Results of our finite element simulations are summarized in Fig. 4. These simulations were performed for a 30 μm diameter cell on a 32 μm x 32 μm electrode.

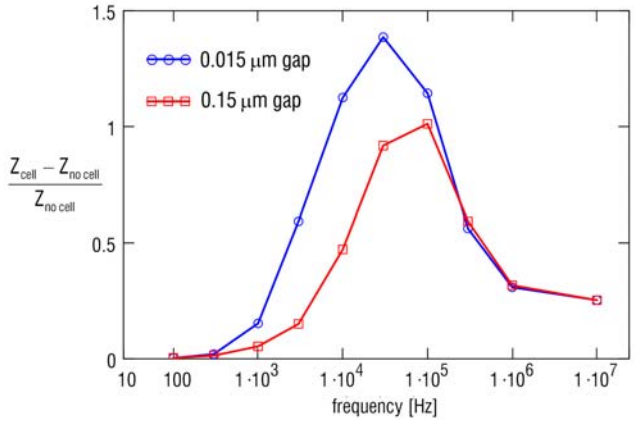

Fig. 4 Normalized impedance change (□) 0.15 μm cell-electrode gap; and (◇) 0.015 μm cell-electrode gap. Frequency is in log scale.

With no cell present, we predict an $f^{-0.9}$ dependence at low frequency (not shown). In Fig. 4 we plot the normalized impedance change $(Z_{cell}-Z_{nocell})/Z_{nocell}$ as a function of frequency. Briefly, the impedance magnitude is essentially unaffected by the cell coverage at very low frequencies as the resistance of the medium in the cell-electrode gap is small compared to the electrode impedance. At moderate frequencies, the impedance magnitude is increased by the presence of cells. At high frequencies, there is essentially no current flow beneath the cells and consequently the spreading resistance determines the impedance. The spreading resistance is weakly dependent on the cell coverage. As a result, plots of the normalized impedance change show a peak with amplitude which depends on cell coverage. The peak frequency is related to the cell-electrode gap and the size of contiguous cell colonies.

ELECTRODE FABRICATION AND METHOD OF IMPEDANCE MEASUREMENT

Gold electrodes were fabricated by a lift-off process. First photoresist was spun on fused silica wafers and patterned using photolithographic technique. About 30 nm of adhesion layer of chromium, followed by 150 nm of gold deposited on the patterned photoresist. The photoresist is then removed and metal not in contact with substrate is then washed away.

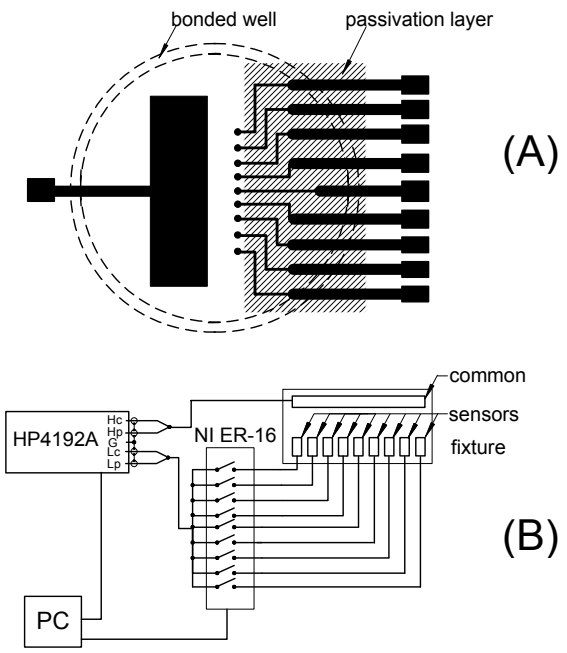

Fig. 5 Schematic presentation of (A) sensor configuration and (B) Impedence measurement set-up.

9 sensing sites with the width of 100 μm and one large counter electrode (area 3.4 mm^2). Epoxy EP30HT (Master Bond, Hackensack, NJ) was painted to cover most of the interconnect metal line. The actual electrode areas are about 0.013 mm^2 were estimated by examining microscopic images. A bottomless plastic wall cut from 48-well culture plate was bonded to the substrate surrounding the 9 sensors and counter electrode (Figure 5A). The well, during impedance measurements, was placed in a homemade environmental chamber maintained at 37^{O}C and 5 – 10% CO_2 in air. Measurements of admittance magnitude (inverse of the impedance) were performed using a Hewlett Packard 4192A admittance meter. 50 mV peak-to-peak AC signal was applied over frequency range 10^2 – 10^6 Hz. Sensing sites were switched using a National Instruments ER-16 relay board (Figure 5B).

IMPEDANCE MEASUREMENT WITHOUT CELLS

0.5 ml of serum free tissue culture medium (Dulbecco's Modified Eagle medium (DMEM), Gibco Laboratories, Grand Island, NY) was added to the cleaned well containing nine sensing sites. Several measurements were made until stabilization was accomplished, which required about 30 - 60 minutes. Six out of nine sensing sites were found to operate properly.

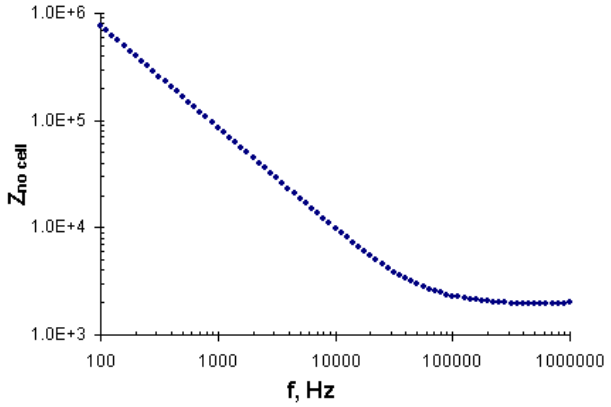

Fig. 6: Electrode impedance magnitude as a function of frequency from 10^2 to 10^6 Hz. Electrode area was estimated mm^2.

Figure 6 shows the measured impedance of one sensing site as function of frequency. At high frequency (10^5 – 10^6 Hz), the measured impedance is constant. In this regime, measured impedance is mostly dominated by spreading resistance. Spreading resistance is proportional to the inverse square root of electrode area, and is independent of frequency. As the frequency is decreased, the impedance increases according to f^{-n}, where n is expected to be between 0.5 to 1. Our measurements show n = 0.94, which is similar to other published values (Onaral & Schwan, 1982; Brokholder, 1998). The impedance at lower frequencies is dominated by diffusive ion transport and capacitive current flow through the double layer at the electrode interface. The measured impedance was inversely proportional to electrode area, which agrees with the literature (Giaever & Keese, 1986; Brokholder, 1998).

IMPEDANCE WITH CELLS – A CELL GROWTH EXPERIMENT

3T3 mouse fibroblasts were maintained in DMEM supplemented with 10% calf serum, 50 units/ml penicillin, 50 μg/ml streptomycin, 2mM L-Glutamine, and 5mM HEPES buffer. The same medium was used to sustain the cells during the impedance experiments. The cells were prepared as a suspension by dislodging cells adhered to a starter culture plate with Trypsin (0.25%). The suspended cells were added into the well containing the sensors at a concentration of $5*10^4$/cm^2 in a final volume of 0.5 ml. The well was placed in homemade environmental chamber that allowed for the cells to be viewed via an electronic probe station microscope while growth conditions were controlled at 37°C and 5-10% CO_2 in air. Impedance measurements were performed every 30 minutes over 24 hours. After 24 hours, the medium was replaced with fresh medium as described above, and controlled incubation continued.

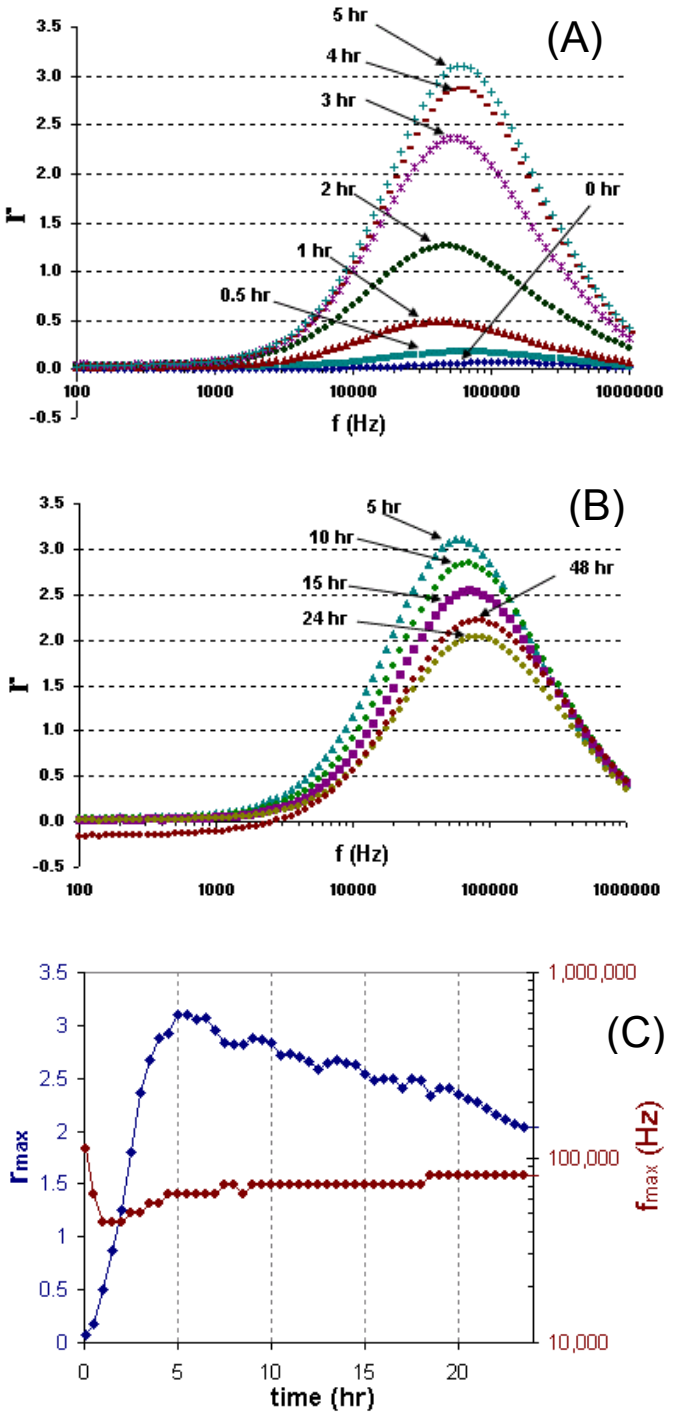

Fig. 7 Plot of normalized impedance change (r) over a range of 10^2 – 10^6 Hz over 48 hours after 3T3 fibroblasts were deposited. 95% to 100% cell coverage on substrate was observed from light microscope. (A) O-5 hours after deposition, (B) 5-48 hours after deposition, and (C) maximum r value (r_{max}) and frequency at r_{max} plotted over 24 hours.

Figures 7A and 7B show how the normalized impedance changed over 48 hours for one sensing site after adding suspended cells. Here, the normalized impedance (*r*) is defined as

$$r = \frac{Z_{cell} - Z_{no\_cell}}{Z_{no\_cell}}$$

Comparable results were obtained for the other sites (not shown).

We observed a peak in intermediate frequency domain (near 10^5 Hz). Figure 7C shows that over the first 4 hours, the peak value of impedance (r_{max}) steadily increased. This observation concurs with our optically-observed changes in cell morphology. Suspended cells typically require around 3-5 hours to be fully spread-out.

The frequency at which the peak value of impedance occurred (f_{max}) was found to initially shift to lower frequency, and then slightly shift to higher frequency. We do not yet fully understand the small shifts in peak frequency. As noted earlier, during the first few hours, the cells typically undergo a morphological change entailing a spherical to spread-out transition. Thus, we hypothesize that the pattern reflects the complex processes of focal adhesion formation and cellular skeleton reorganization.

Figure 7B also shows a slightly decrease in impedance at 48 hours ($r < 0$) at *low* frequency (100 – 1000 Hz). We attribute the observed decrease to the adsorption of cellular proteins and other products. When proteins or other cellular products absorb on the electrode surface, the isoelectric point of the surface shifts. Because, many proteins have a net negative charge, the positive ion concentration may increase near the surface. Consequently, the interfacial capacitance (C_I) and Warburg impedance (Z_W) will decrease. Since C_I and Z_W dominate the measurement at low frequency, the total impedance at low frequency can thus decrease.

CONCLUSIONS

We have observed that as cells adhere and proliferate on sensing electrodes, the impedance at intermediate frequencies monotonically increases over the first 5 hours. From other experiments, we have observed that 5 hours is also required for a similarly concentrated suspension of cells to spread-out and fully cover a surface. Moreover, no significant cells growth occurred over 48 hours because the concentrated suspension essentially yielded a confluent cell culture once cell spreading was complete.

Based on analytic theory (Giaever & Keese, 1981) and our simulations, the results indicate that cell surface coverage area on the electrode and cell-substrate gap distance are associated with current blockage and thus, the measured value of impedance. There appears to be consistency between biological events and the electrical measurements. Namely, as cells settle from suspension and associate with the surface, focal adhesion contacts are formed (reduced cell-surface gap) and spreading (increased area coverage) occur.

From the technological perspective, arrays of impedance sensors could play a role in automating cell proliferation assays. Further work may indicate that the different adhesion profiles and extents that different cell types exhibit could be discerned with impedance measurements. Finally, apoptosis assays could also prove to be a useful application for impedance sensing arrays.

ACKNOWLEDGMENTS

This publication is based upon work supported by the National Science Foundation under Grant No. ECS-0088520. Any opinions, findings, and conclusions or recommendations expressed in this material are those of the authors and do not necessarily reflect the views of the National Science Foundation. MMD thanks Automated Cell Inc. of Pittsburgh PA for their initial assistance with acquiring different cell lines.

REFERENCES

1. Borkholder D. Cell Based Biosensors Using Microelectrodes, Ph.D. dissertation, Stanford University, Palo Alto (1998).
2. Ehret R. et al. Monitoring of cellular behaviour by impedance measurements on interdigitated electrode structures. Biosensors & Bioelectronics 12, 29-41 (1997).
3. Huang X., Nguyen D., Greve D.W., & Domach M.M. Microelectrode impedance changes due to cell growth: simulation and measurement (submitted IEEE Sensor, 2003).
4. Giaever I. & Keese C.R. Use of electric fields to monitor the dynamical aspect of cell behavior in tissue culture. IEEE Transactions on Biomedical Engineering, BME-33(2), 242-247 (1986).
5. Giaever I. & Keese C.R. Micromotion of mammalian cells measured electrically. Proc. Natl. Acad. Sci. 88, 7896-7900 (1991).
6. Onaral B. & Schwan H.P. Linear and nonlinear properties of platinum electrode polarization. Part 1: frequency dependence at very low frequencies. Med. & Biol. Eng & Comput., 20, 299-306 (1982).

7. Tiruppathi C. et al. Electrical method for detection of endothelial cell shape change in real time: assessment of endothelial barrier function. Proc. Natl. Acad. Sci. 89, 7919-7923 (1992).

CONTACT

Michael M. Domach; email: md0q@andrew.cmu.edu